Backstepping Control of Double Star Synchronous Machine Fed by Two Three-Level Inverters

Elakhdar BENYOUSSEF, Abdelkader MEROUFEL
Faculty of Science and Engineering, Department of Electrical Engineering, University of Djilali Liabes, Sidi Bel Abbes 22000, BP 89 Algeria, Intelligent Control Electronic Power System laboratory (ICEPS)
Corresponding author :lakhdarbenyoussef@yahoo.com

Said BARKAT
Faculty of Science and Engineering, Department of Electrical Engineering, M'sila University, Ichbilia Street, M'sila 28000, Algeria

Abstract–*This work relates to the study of backstepping control of the salient-pole double star synchronous machine drive fed by two three-level inverters. Indeed, it is a question of carrying out a decoupling between stator current and electromagnetic torque, by introducing a backstepping control with an optimal torque working and by imposing constant flux regime. Furthermore, to ensure a decoupled dynamic behaviour of the machine as in the case of a DC machine, a control of the rotor current has been introduced through a buck converter, feeding the excitation circuit. The obtained results are very satisfactory and reveal the effectiveness of the proposed approach.*

Key words: *Double Star Synchronous Machine; Multilevel Inverter; Space Vector Modulation; Backstepping Control.*

1. Introduction

Multiphase drives possess several advantages over conventional three-phase drives such as reducing the amplitude of torque pulsations, reducing the amplitude, and increasing the frequency of torque pulsation, and improving noise characteristics [1]. The multiphase machines drives are widely used in electrical ships, aircraft, locomotive traction, electric and hybrid vehicles. Recently, special attention is focused on the double star machine drive systems. In double star machine two sets of three-phase windings spatially phase shifted by 30 electrical degrees are implemented in the same stator. Two common examples of such structures are the double star induction machine and double star synchronous machine (DSSM).

It is well known that the variable speed double star drives require two traditional PWM inverters. Commonly, it is difficult to achieve clean output waveform using two-level inverters. Indeed, current harmonics caused by no sinusoidal voltage feeding imply power losses in switching elements, necessity of using special filters for high frequency components in the output voltages, and pulsating torques in multiphase drives. These drawbacks can be lowered using multilevel inverters.

Multilevel inverter topology can offer reduced harmonic distortions of the output currents, low voltage stresses of power switches and reduced electromagnetic interferences [2]. Therefore, it is a preferred solution for medium-high voltage or high-power electrical drives applications. Many multilevel topologies have been developed, among them, the neutral-point clamped (NPC).As reported in the literature, numerous PWM strategies have been proposed to control this kind of inverter. The space vector modulation (SVM) technique is one of the well-known modulation methods. SVM offers approximately a round rotary magnetic field by switching the stator voltage space vectors. Then, it can improve the voltage efficiency, quicken the dynamic responses and reduce the torque ripples of an electrical drive even at low switching frequency.

In other hand, the DSSM is basically a nonlinearly coupling system which leads to a challenging control task. Indeed, traditional control methods such as PI control are not suitable for high performance drive applications. To ease these difficulties, various control algorithms have been advised in the literature. Among them, nonlinear state feedback control [3], sliding mode control [4] ….Backstepping control theory is one of the prospective control methodologies for electrical drives. It can offer many good properties, such as systematically approach with few control parameters and the ability to shape performance. The backstepping technique has been widely used in the design of speed controllers for induction motors [5][6][7] and permanent magnet motors [8][9][10][11].

The main purpose of this paper is to apply the backstepping control on DSSM fed by two three-level NPC inverters controlled by three-level space vector modulations.

The present paper is organized as follows. In Section II, the double star synchronous machine model is reported. Section III details the SVM algorithm for three-level NPC inverter. The backstepping control scheme is proposed in Section IV. Results and discussion are submitted in Section V. The conclusion is given in the last section.

2. Modelling of the double star synchronous machine

As every rotating electrical machine, the double star synchronous machine is composed of a stator and rotor. Thus, the machine windings can be substituted by an equivalent scheme in the (d,q). The dynamic model of a double star synchronous machine can be described in the d-q frame as follows:

$$\begin{cases} \dfrac{di_d}{dt} = -\dfrac{R}{L_d} i_d + \omega \dfrac{L_q}{L_d} i_q + \dfrac{1}{L_d} v_d \\ \dfrac{di_q}{dt} = -\dfrac{R}{L_q} i_q - \omega \left(\dfrac{L_d}{L_q} - \dfrac{M_{fd}^2}{L_q L_f} \right) i_d + \omega \dfrac{M_{fd}}{L_q L_f} \phi_f + \dfrac{1}{L_q} v_q \\ \dfrac{d\phi_f}{dt} = -\dfrac{R_f}{L_f} \phi_f + \dfrac{M_{fd} R_f}{L_f} i_d + v_f \\ \dfrac{d\Omega}{dt} = (a_1 i_d + a_2 \phi_f) i_q - \dfrac{T_L}{J} - \dfrac{f}{J} \Omega \end{cases} \quad (1)$$

Where

$$a_1 = \frac{p}{J}\left(L_d - L_q - \frac{M_{fd}^2}{L_f} \right); \quad a_2 = \frac{pM_{fd}}{JL_f}$$

Where v_d and v_q are the *d-q* axis stator voltages; v_f rotor excitation voltage; i_d and i_q are the *d-q* axis stator currents; i_f rotor excitation current; L_d and L_q are the *d-q* axis stator inductances; L_f rotor excitation inductance; R is the stator resistance; R_f is the rotor resistance; p is the number of pole pairs; f is the viscous friction coefficient; T_L is the load torque; Ω is the rotor speed and J is the rotor moment of inertia.

Figure 1 represents the backstepping control of double star synchronous machine.

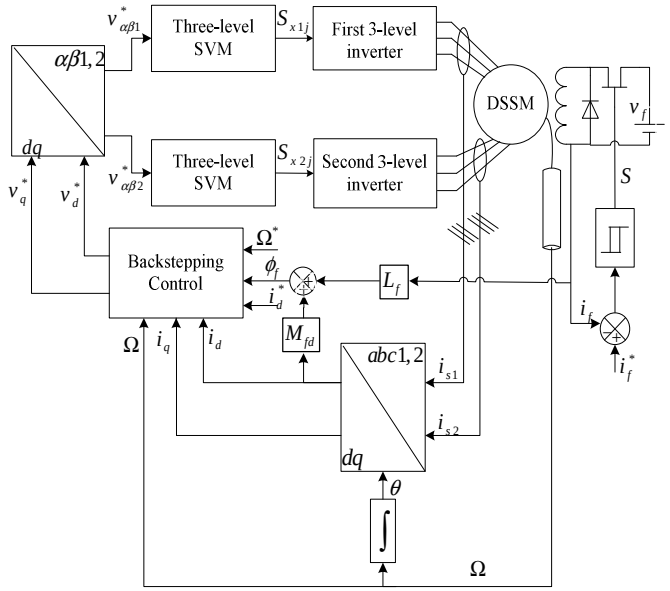

Fig. 1. Backstepping control of DSSM (with *j=1, 2* and *x=a, b, c*)

Transformation between *dq* and $\alpha\beta$ frames for first and second star is given by:

$$\begin{cases} \begin{pmatrix} v_{\alpha 1}^* \\ v_{\beta 1}^* \end{pmatrix} = \begin{pmatrix} \cos(\theta) & -\sin(\theta) \\ \sin(\theta) & \cos(\theta) \end{pmatrix} \begin{pmatrix} v_d^* \\ v_q^* \end{pmatrix} \\ \begin{pmatrix} v_{\alpha 2}^* \\ v_{\beta 2}^* \end{pmatrix} = \begin{pmatrix} \cos(\theta - \gamma) & -\sin(\theta - \gamma) \\ \sin(\theta - \gamma) & \cos(\theta - \gamma) \end{pmatrix} \begin{pmatrix} v_d^* \\ v_q^* \end{pmatrix} \end{cases} \quad (2)$$

With $\gamma = \pi/6$ and θ : is rotor position.

Transformation between the six-phase system and two-phase system is carried out using the flowing equation:

$$\begin{cases} \begin{pmatrix} i_\alpha \\ i_\beta \end{pmatrix} = [T] \begin{pmatrix} i_{abc1} \\ i_{abc2} \end{pmatrix} \\ \begin{pmatrix} i_d \\ i_q \end{pmatrix} = \begin{pmatrix} \cos(\theta) & \sin(\theta) \\ -\sin(\theta) & \cos(\theta) \end{pmatrix} \begin{pmatrix} i_\alpha \\ i_\beta \end{pmatrix} \end{cases} \quad (3)$$

Where the matrix *T* is given by:

$$[T] = \frac{1}{\sqrt{3}} \begin{bmatrix} \cos(0) & \cos\left(\frac{2\pi}{3}\right) & \cos\left(\frac{4\pi}{3}\right) & \cos(\gamma) & \cos\left(\frac{2\pi}{3}+\gamma\right) & \cos\left(\frac{4\pi}{3}+\gamma\right) \\ \sin(0) & \sin\left(\frac{2\pi}{3}\right) & \sin\left(\frac{4\pi}{3}\right) & \sin(\gamma) & \sin\left(\frac{2\pi}{3}+\gamma\right) & \sin\left(\frac{4\pi}{3}+\gamma\right) \end{bmatrix} \quad (4)$$

3. SVM for three-level inverter

The three-level NPC voltage inverter consists of twelve pairs of transistors-diodes and six clamping diodes as shown in figure 2. The simple voltage of each phase is entirely defined by the state of the four transistors constituting each arm. The median diodes of each arm permits to have the zero level of the inverter output voltage. Only three sequences of operation are retained and done in work. Each arm of the inverter is modeled by a perfect switch with three positions (0, 1, and 2) [12].

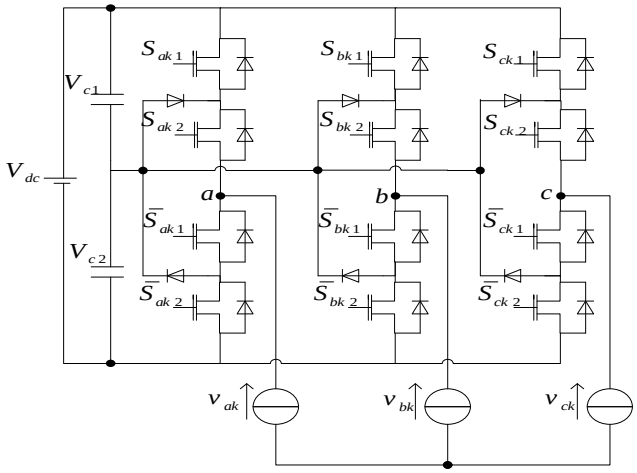

Fig. 2. Schematic diagram of a three-level inverter with (*k*=1 for the first inverter 1 and *k*=2 for the second inverter 2)

Now, considering the *m* states (m = 2, 1, 0) of each arm, the three-level inverter has a total of m^3 possible combinations of switching states. As a result, 27 vectors can construct the space-vector diagram of a three-level converter, shown as figure 2. There are 24 active vectors including 12 short vectors, 6 medium vectors and 6 long vectors, and the remaining three are zero vectors.

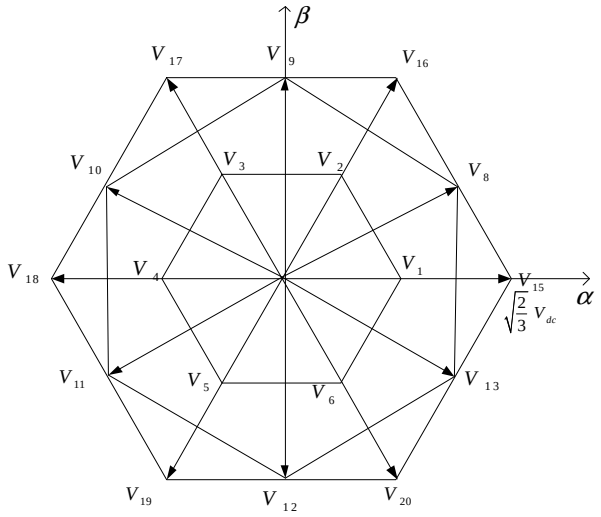

Fig. 3. Three-level voltage inverter vectors in the α-β frame.

The small hexagon (figure 3.a), is defined by the six regions I, II, III, IV, V, and VI. All vectors limiting these regions have the same magnitude $V_{dc}/\sqrt{6}$.

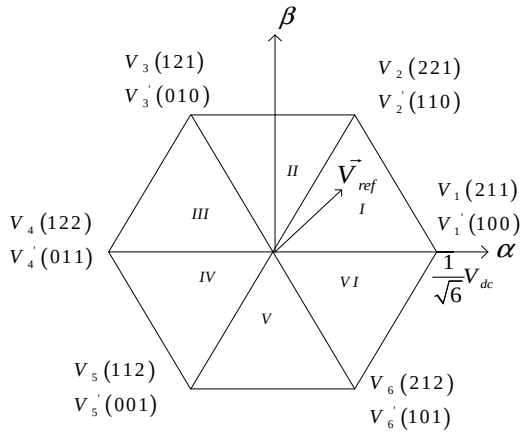

Fig. 3.a. Three-level inverter small hexagon.

The middle hexagon (figure 3.b)is defined by the six regions a, b, c, d, e, and f. All vectors limiting these regions have the same magnitude $V_{dc}/\sqrt{2}$.

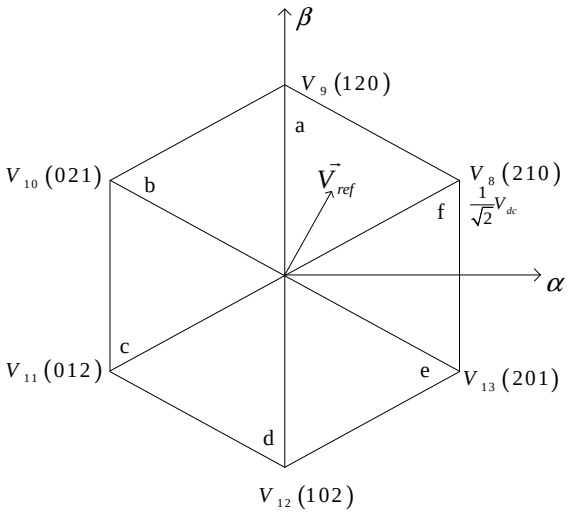

Fig. 3.b. Three-level inverter middle hexagon.

The big hexagon (figure 3.c) is defined by the six regions A, B, C, D, E, and F. All vectors limiting these regions have the same magnitude $\sqrt{2/3}\ V_{dc}$.

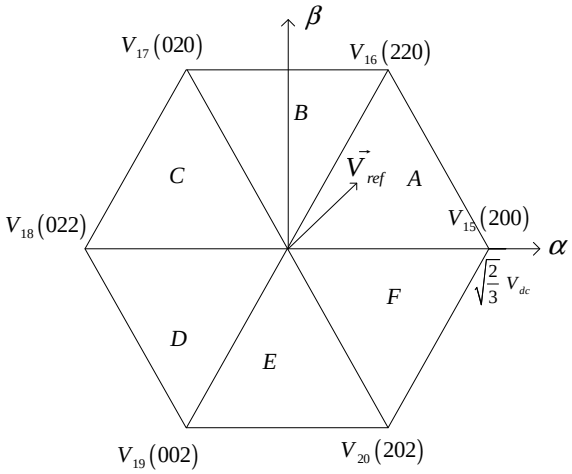

Fig. 3.c. Three-level inverter big hexagon.

Several strategies are proposed in order to generate the inverter's gates pulses. In this work, we used the space vector modulation (SVM) is adopted. In this topic, the principle and the description of the SVM strategy will be detailed and applied to the three-level voltage.

A. Principle

As shown on figures3.a,b,c in each of the three hexagons, the reference vector V_{ref} is located in one of the six regions constituting the hexagon, where each region is limited by two adjacent vectors $V_\delta$et $V_{\delta+1}$ (figure 4).

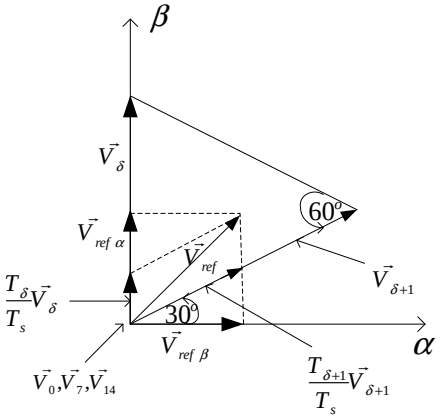

Fig. 4. A typical region of 3-level space vector diagram

Then V_{ref} is equal to:

$$\begin{cases} \vec{V}_{ref} = \dfrac{T_\delta}{T_s}\vec{V}_\delta + \dfrac{T_{\delta+1}}{T_s}\vec{V}_{\delta+1} + \dfrac{T_0}{T_s}\vec{V}_z \\ T_0 = T_s - T_\delta - T_{\delta+1} \end{cases} \quad (5)$$

Where T_s is the sampling time, T_δ, $T_{\delta+1}$ are the application times of V_δ and $V_{\delta+1}$ respectively. In one sample time, V_{ref} is equal to V_δ during T_δ and $V_{\delta+1}$ during $T_{\delta+1}$. In the rest of T_s,

V_{ref} is equal to the zero vector V_z (V_{14}, V_0, and V_7) during T_0 following this optional choice: V_{14}, V_0 at the pulse's ends and V_7 at the pulse's centre. At the same time:

$$\vec{V}_{ref} = \vec{V}_{ref\,\alpha} + \vec{V}_{ref\,\beta} \tag{6}$$

Or, in complex writing:

$$V_{ref} = \sqrt{V_{ref\,\alpha}^2 + V_{ref\,\beta}^2}\, e^{j\varphi} \tag{7}$$

Where φ is an angle varying from 0 to 2π.

The SVM pulse is symmetrical and where all switches of the inverter's half-bridge have the same state in the center and in the two ends. So, following these properties and after calculation of T_δ, $T_{\delta+1}$and T_0 of each region belonging to the appropriate hexagon, the pulses of the higher half-bridge ($S_{x1}, S_{x2},\ x = a,b,c$) of the three-level inverter are build.

B. Switching times calculation

As said previously, there are three hexagons as shown in figure3, where each one is constituted of six regions. As a result, 18 regions require switching times computation. To simplify this task, and for reason of similarities in the six regions of one hexagon on the one hand, and resemblance between hexagons 'a' and 'c' on the other hand (the largest magnitude in hexagon 'a' $V_{dc}/\sqrt{6}$ constitutes the half of the largest magnitude in hexagon 'c' $V_{dc}\sqrt{2/3}$, for these all reasons, in the switching times calculation's procedure, only two regions of hexagon 'a' and hexagon 'b', are considered. The other switching times will be then deduced from these four regions.

- Region I switching time's calculation:

Figure (5) presents the different voltage vectors forming the region I.

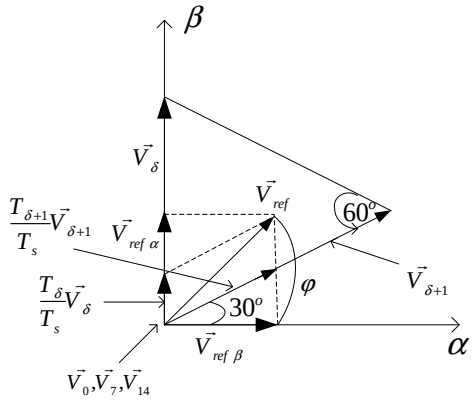

Fig. 5. Switching times calculation.

The reference voltage vector could be expressed using three vectors when it lies in any region. After projection, it is possible to find:

$$\begin{cases} V_{ref\,\alpha} = \dfrac{T_1}{T_s}V_1 + \dfrac{T_2}{T_s}V_2 \sin\left(\dfrac{\pi}{6}\right) \\ V_{ref\,\beta} = \dfrac{T_2}{T_s}V_2 \cos\left(\dfrac{\pi}{6}\right) \end{cases} \tag{8}$$

The switching times applied for each vector are shown below:

$$\begin{cases} T_1 = \dfrac{\sqrt{6}V_{ref\,\alpha} - \sqrt{2}V_{ref\,\beta}}{E} T_s \\ T_2 = \dfrac{2\sqrt{2}V_{ref\,\beta}}{E} T_s \\ T_0 = T_s - T_1 - T_2 \end{cases} \tag{9}$$

C. Examples of chronograms

Figure 6 illustrates the pulses of region 'I'. It is about symmetrical signals that have the same states at the center and at the ends.

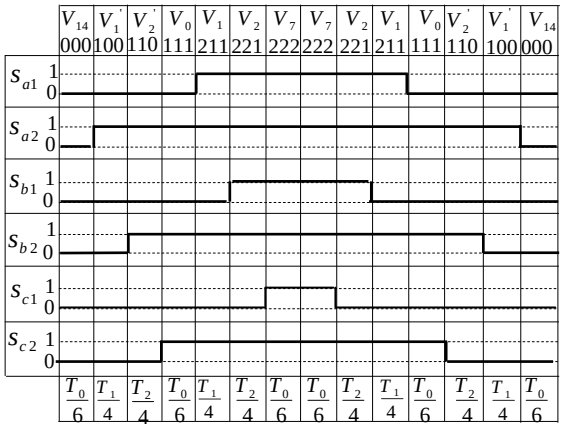

Fig. 6. Examples of chronograms pulses of region I

4. Backstepping control

The idea of backstepping design is conducted to select recursively some appropriate functions of the state variables of the machine to be controlled. In this work, the speed and direct stator current are assumed as pseudo-control inputs for lower dimension subsystems of the overall system. The backstepping procedure is ended when the control feedback design highlights the real physical input. Hence, it results that the final Lyapunov function is found from all associated Lyapunov functions defined for each individual design step [6].

A. Step 1

This first step consists in identifying the error e_Ω which representing the error between real speed Ω and its reference Ω^*. The speed error is identified by:

$$e_\Omega = \Omega^* - \Omega \tag{10}$$

The error dynamic is given by

$$\dot{e}_{\Omega} = \dot{\Omega}^{*} - \left(\left(a_1 i_d + a_2 \phi_f \right) i_q - \frac{T_L}{J} - \frac{f}{J} \Omega \right) \tag{11}$$

The first Lyapunov candidate V_1 is chosen as

$$V_1 = \frac{1}{2} e_{\Omega}^2 \tag{12}$$

To have a convergence of the error e_{Ω} to ward zero, it is necessary that the Lyapunov function derivative $\dot{V}_1$ is negative, which will allow the following choice.

$$\dot{e}_{\Omega} = -k_{\Omega} e_{\Omega} \tag{13}$$

Taking the time derivative of V_1, this leads to

$$\dot{V}_1 = -k_{\Omega} e_{\Omega}^2 < 0 \tag{14}$$

Thus, the tracking objectives will be satisfied using the following control law

$$i_q^{*} = \frac{1}{a_1 i_d + a_2 \phi_f} \left(\dot{\Omega}^{*} + k_{\Omega} e_{\Omega} + \frac{T_L}{J} + \frac{f}{J} \Omega \right) \tag{15}$$

So, the control i_q^{*} is asymptotically stable.

B. Step 2

The second step consists in identifying the errors e_{id} and e_{iq} which represent the errors signals between the currents and theirs references currents. Let us define the current errors as follows:

$$\begin{cases} e_{id} = i_d^{*} - i_d \\ e_{iq} = i_q^{*} - i_q \end{cases} \tag{16}$$

On the other hand, Eq. (15, 16) can be expressed as

$$\dot{e}_{\Omega} = \begin{bmatrix} -k_{\Omega} & 0 & \left(a_1 i_d + a_2 \phi_f \right) \end{bmatrix} e \tag{17}$$

With: $e = \begin{bmatrix} e_{\Omega} & e_{id} & e_{iq} \end{bmatrix}^T$

The errors dynamics are given by

$$\begin{cases} \dot{e}_{id} = \dot{i}_d^{*} - f_1(x) - \frac{1}{L_d} v_d \\ \dot{e}_{iq} = \dot{i}_q^{*} - f_2(x) - \frac{1}{L_q} v_q \end{cases} \tag{18}$$

With

$$\begin{cases} f_1(x) = -\frac{R}{L_d} i_d + \omega \frac{L_q}{L_d} i_q \\ f_2(x) = -\frac{R}{L_q} i_q - \omega \left(\frac{L_d}{L_q} - \frac{M_{fd}^2}{L_q L_f} \right) i_d + \omega \frac{M_{fd}}{L_q L_f} \phi_f \end{cases}$$

Since, in the errors dynamics expressions (18) of the stator current components, the actual control inputs (v_d, v_q) have appeared and will be calculated. Stability analysis is done by:

$$V_2 = \frac{1}{2} e_{\Omega}^2 + \frac{1}{2} e_{id}^2 + \frac{1}{2} e_{iq}^2 \tag{19}$$

Taking the time derivative of V_2 and using (17), this yields to

$$\begin{aligned} \dot{V}_2 = & -k_{\Omega} e_{\Omega}^2 + e_{id} \left(\dot{i}_d^{*} - f_1(x) - \frac{1}{L_d} v_d \right) \\ & + e_{iq} \left(\dot{i}_q^{*} - f_2(x) - \frac{1}{L_q} v_q + \left(a_1 i_d + a_2 \phi_f \right) e_{\Omega} \right) \end{aligned} \tag{20}$$

At last, in order to make the derivative of the complete Lyapunov function (20) be negative definite, the *d*-axis and *q*-axis voltages control inputs are chosen as follows:

$$\begin{cases} v_d^{*} = L_d \left(\dot{i}_d^{*} - f_1(x) + k_{id} e_{id} \right) \\ v_q^{*} = L_q \left(\dot{i}_q^{*} - f_2(x) + \left(a_1 i_d + a_2 \phi_f \right) e_{\Omega} + k_{iq} e_{iq} \right) \end{cases} \tag{21}$$

5. Simulation results

The proposed backstepping control of the double star synchronous machine supplied by two NPC three-level voltage source inverters controlled via space vector modulation strategy is tested by digital simulation.

Figure 7 presents the dynamic response of electrical drive. To test the speed evolution of the system, the DSSM is accelerate from standstill to reference speed *100rad/s* with a load variation of *11Nm* to *0Nm* between *0.8*s and *1.2*sfollowed by a speed inversion from *100rad/s* to-*100*rd/s at *1.5*s.

The proposed control performances are very satisfactory. The rejection of disturbance is very efficient. Note that the i_d current is maintained null and independent of the torque; the i_q current reflects the picture of the electromagnetic torque. The decoupling is ensured for the nominal load. This control decreases considerably the torque ripples. It can be seen that the speed response is merged with the reference case after wards the response time t_r*=0.16*s.

From these simulation results, one can say that the proposed backstepping control presents an excellent performance for starting, rejection of disturbance and decrease considerably the torque ripples.

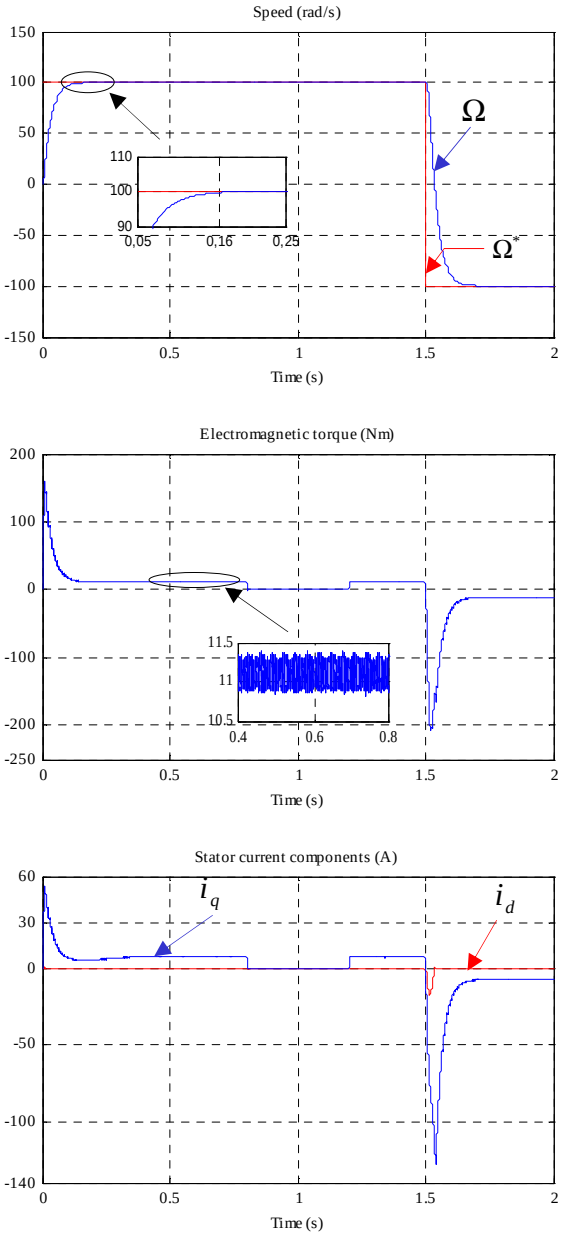

Fig. 7. Dynamic responses of DSSM controlled by backstepping method in the case of a torque variation followed by a speed reversion

6. Conclusion

In this paper, a nonlinear feedback controller based on a backstepping method for a double star synchronous machine has been developed. To achieve global asymptotic stability of the proposed controller, Lyapunov theory is applied. Some simulation results were carried out to illustrate the effectiveness of the proposed control system. It is pointed out that the robustness of the controlled double star synchronous machine drive against speed and load torque variations is guaranteed. Furthermore, the proposed control scheme decreases considerably the torque ripples and assures good speed tracking without overshoot. The decoupling between the direct current and the torque is maintained, confirming the good dynamic performances of the developed drive systems.

7. Appendix

Double star synchronous machine parameters are gathered in Table. 1.

Table 1: DSSM Parameters.

DSSM, 5kW, 2 poles, 232V, 50 Hz	
Stator resistance (R_s)	2.35 Ω
Rotor resistance (R_f)	30.3 Ω
Stator inductance d axis (L_d)	0.3811H
Rotor inductance q axis (L_q)	0.211H
Stator inductance (L_f)	15 H
Mutual inductance (M_{fd})	2.146 H
Total inertia (J)	0.05Nms^2/rad
Friction coefficient (f)	0.001Nms/rad

8. References

[1] Sadouni, R., Meroufel, A.: *Indirect Rotor Field-oriented Control (IRFOC) of a Dual Star Induction Machine (DSIM) Using a Fuzzy Controller*. In: Acta Polytechnica Hungarica, Vol. 9, No. 4, 2012, p. 177- 192.

[2] Nezli, L. Mahmoudi, M.: *Vector Control with Optimal Torque of a Salient–Pole Double Star Synchronous Machine Supplied Fed by Three–Level Inverters*. In: Journal of Electrical Engineering, Vol. 61, No. 5, 2010, p. 257-263.

[3] Massoum, A. Fellah, M. Meroufel, A. Bendaoud, A.: *Input Output Linearization and Sliding Mode Control of a Permanent Magnet Synchronous Machine Fed by a Three-Level Inverters*. In: Journal of Electrical Engineering, Vol. 57, No.4, 2006, p. 205-210.

[4] Massoum, A. Meroufel, A. Bentaallah A.: *Sliding Mode Speed Controller for a Vector Controlled Double Star Induction Motor*. In.: Electrical Review, 2012, p. 205-209.

[5] Trabelsia, R. Khedherb, A. Mimounic, M. M'sahli, F.: *Backstepping Control for an Induction Motor Using an Adaptive Sliding Rotor Flux Observer*. In: Electric Power Systems Research, Vol. 93, 2012, p. 1-15.

[6] Chaouch, S. Nait-Said, M. Makouf, A. Cherifi, L.: *Backstepping Control Based on Lyapunov Theory for Sensorless Induction Motor with Sliding Mode Observer*. In: Ariser Journal-Sciences, Vol. 4, No. 1, January 2008, p. 19-27.

[7] Hwang, Y. Park, K. Yang, H.: *Robust Adaptive Backstepping Control for Efficiency Optimization of Induction Motors with Uncertainties*. In: IEEE International Symposium on Industrial Electronics, 2008, p. 878-883.

[8] Xie, Q. Han, Z. Kang, H.: *Adaptive Backstepping Control for Hybrid Excitation Synchronous Machine with Uncertain Parameters*. In: Expert Systems with Applications, Vol. 37, 2010, p. 7280-7284.

[9] Jinpeng, Y. Haisheng, B. Junwei Gao, Y.: *Adaptive Fuzzy Tracking Control for the Chaotic Permanent Magnet Synchronous Motor Drive System via Backstepping*. In: Nonlinear Analysis: Real World Applications, Vol. 12, 2011, p. 671-681.

[10] Karabacak, M. Eskikurt, H.: *Design, Modelling and Simulation of a New Nonlinear and full Adaptive Backstepping Speed Tracking Controller for Uncertain PMSM*. In: Applied Mathematical Modelling Vol. 36, 2012, p. 5199-5213.

[11] Karabacak, M. Eskikurt, H.: *Speed and Current Regulation of a Permanent Magnet Synchronous Motor via Nonlinear and Adaptive Backstepping Control*. In: Mathematical and Computer Modelling Vol. 53, 2011, p. 2015-2030.

[12] Panda, A. Suresh, Y.: *Research on Cascade Multilevel Inverter with Single DC Source by Using Three-Phase Transformers*. In: International Journal Electric Power Energy System, Vol. 40, No. 1, 2012, p. 9-20.